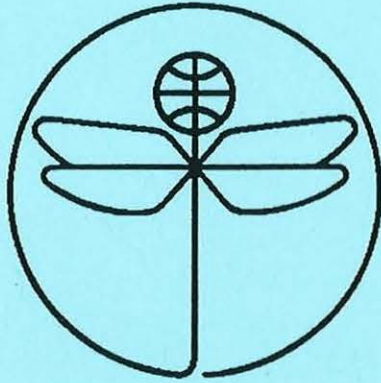


TWENTY FIRST EUROPEAN ROTORCRAFT FORUM



Paper No I.3

**THE HIGH SPEED IMPULSIVE NOISE PREDICTION
THROUGH A VOLUME INTEGRATION:
THE PROBLEM OF MULTIPLE EMISSION TIMES**

BY

S. Ianniello, E. De Bernardis

CIRA, Italian Aerospace Research Center
CAPUA, ITALY

August 30 - September 1, 1995
SAINT - PETERSBURG, RUSSIA

Paper nr.: I.3



The High Speed Impulsive Noise Prediction Through a Volume Integration:
The Problem of Multiple Emission Times.

S. Ianniello; E. De Bernardis

TWENTY FIRST EUROPEAN ROTORCRAFT FORUM

August 30 - September 1, 1995 Saint-Petersburg, Russia

THE HIGH SPEED IMPULSIVE NOISE PREDICTION THROUGH A VOLUME INTEGRATION: THE PROBLEM OF MULTIPLE EMISSION TIMES

S. Ianniello and E. De Bernardis

C.I.R.A.,

Italian Aerospace Research Center

Capua, Italy

Abstract

The problem of the HSI noise prediction from rotating blades is treated through a volume integration, following the so called *acoustic analogy approach*. Two different solution forms are adopted, moving the integration domain from the computational grid to its own acoustic image, to bypass the numerical singularities in the integral kernels. The problem of multiple emission times and the subsequent decomposition of the acoustic volume into three separate supersonic regions is addressed, trying to point at some possible numerical solution. Then a brief discussion about the methodology is proposed, trying to point out the advantages and the perspectives of this particular numerical approach.

1. Introduction

Although a great deal of theoretical and computational work has been carried out over the last few years, a reliable evaluation of noise from helicopter rotors with blade tip speed in the high transonic range is still to be achieved. Both theoretical and numerical tools cannot be considered at an ultimate stage, and the task of providing effective prediction codes for calculating the sound field of helicopters has not yet accomplished. Recently, the Ffowcs Williams-Hawkings equation has been successfully applied for the prediction of HSI noise [1, 2]: through the knowledge of the fluid velocity field around the body and a full three dimensional integration, the computation of the quadrupole noise signature has been achieved for hovering rotor blades at different tip Mach numbers. This method seems to be a valid alternative to the direct use of CFD codes [3, 4, 5] and to the so-called *Kirchhoff's approach* [6, 7, 8, 9], which, at present, are widely used for the aeroacoustic analysis of high speed rotating blades. Anyhow, a lot of numerical problems are related to the volume integration. If the computational grid includes some source points around the sonic circle, the presence of a numerical singularity in the integral kernels (related to the Doppler factor $|1 - M_r|$) may cause a completely unreliable prediction of the acoustic signature. Then, an alternative formulation may be adopted [10], performing the integration on the *acoustic image* of the computational grid: in this manner, the information concerning the retarded time and the Doppler factor are included inside the integration domain, where each source point is considered at its own emission time, avoiding the integrals divergence. However, when a high rotational speed is involved, the shock delocalization phenomena (taking place in the flow field at tip Mach numbers over 0.88), force to account for a grid region off the sonic circle, where the presence of multiple emission times for the supersonic source points causes the decomposition of the acoustic volume into three different patches. The computation of the integrals upon these particular regions is a very difficult problem to be numerically solved, due to the subsequent changes of shape and size of the integration domains. Aim of this paper is to address (and partially solve) these particular problems, whose numerical solution should

supply a reliable prediction of the quadrupole noise signature and, at the same time, an interesting description of the acoustic phenomena taking place in the flow field.

2. Theoretical and numerical aspects

The theoretical basis of our formulation is the well known Ffowcs Williams-Hawkings equation, where the acoustic pressure field generated by a moving body is expressed as the sum of three different contributions, known as *thickness*, *loading* and *quadrupole* noise:

$$\square^2 p' = \frac{\partial}{\partial t} [\rho_0 v_n \delta(f)] - \frac{\partial}{\partial x_i} [\tilde{P}_{ij} \hat{n}_j \delta(f)] + \frac{\partial^2}{\partial x_i \partial x_j} [T_{ij} H(f)] \quad (1)$$

Now our attention is focused on the non linear term on the right-side of equation (1), whose evaluation generally requires the knowledge of the fluid velocity field around the blade, since the presence of the Lighthill stress tensor: $T_{ij} = P_{ij} + \rho u_i u_j - c_0^2 \rho \delta_{ij}$; here ρ is the local air density, u_i is the velocity of the air flow, c_0 the speed of sound in the undisturbed medium, and P_{ij} the compressive stress tensor ($P_{ij} = p \delta_{ij} - \Sigma_{ij}$, with Σ_{ij} the viscous stress tensor). By the use of the Green's function method, the equation (1) is generally turned into an integral form, where the acoustic pressure from the quadrupole source term p_Q is expressed by:

$$\begin{aligned} 4\pi p_Q(\mathbf{x}, t) &= \frac{1}{c_0^2} \frac{\partial^2}{\partial t^2} \iiint_V \left[\frac{T_{rr}}{r|1-M_r|} \right]_{\tau^*} dV \\ &+ \frac{1}{c_0} \frac{\partial}{\partial t} \iiint_V \left[\frac{3T_{rr} - T_{ii}}{r^2|1-M_r|} \right]_{\tau^*} dV \\ &+ \iiint_V \left[\frac{3T_{rr} - T_{ii}}{r^3|1-M_r|} \right]_{\tau^*} dV \end{aligned} \quad (2)$$

Note that all the quantities in the integral kernels must be evaluated at the *retarded* time τ^* , which represents, at each source point, the instant when the contribution to the acoustic pressure field started to reach the observer location \mathbf{x} at the actual observer time t . In the equation (2) the domain V represents the numerical grid, where the knowledge of the fluid velocity components allows the evaluation of the integral kernels, and the presence of the Doppler factor $|1 - M_r|$ points out the relationship between the observer time and location and the kinematics of the rotating blade. For the source points close to the sonic circle M_r easily approaches one, causing the integrals to diverge. This mathematical singularity may be avoided through the introduction of the Doppler factor inside the integration domain, and the adoption of the following solution form:

$$\begin{aligned} 4\pi p_Q(\mathbf{x}, t) &= \frac{1}{c_0^2} \frac{\partial^2}{\partial t^2} \iiint_V \left[\frac{T_{rr}}{r} \right]_{\tau^*} dV \\ &+ \frac{1}{c_0} \frac{\partial}{\partial t} \iiint_V \left[\frac{3T_{rr} - T_{ii}}{r^2} \right]_{\tau^*} dV \\ &+ \iiint_V \left[\frac{3T_{rr} - T_{ii}}{r^3} \right]_{\tau^*} dV \end{aligned} \quad (3)$$

In this equation the integration domain V represents the acoustic image of the numerical grid, where each source point is considered, fixed an observer time and location, at the corresponding emission time τ^* . Since the presence of the source point-observer distance r in the denominator of all kernels, the integrals of equation (3) can never diverge: however, the absence of the numerical singularity must be paid with

the subdivision of the integration domain in the supersonic regions, where multiple emission times may arise at some particular azimuthal positions during the revolution period. Figure 1 shows the quadrupole noise signatures computed with the equations (2) and (3), adopting a different spanwise extension of the numerical grid.

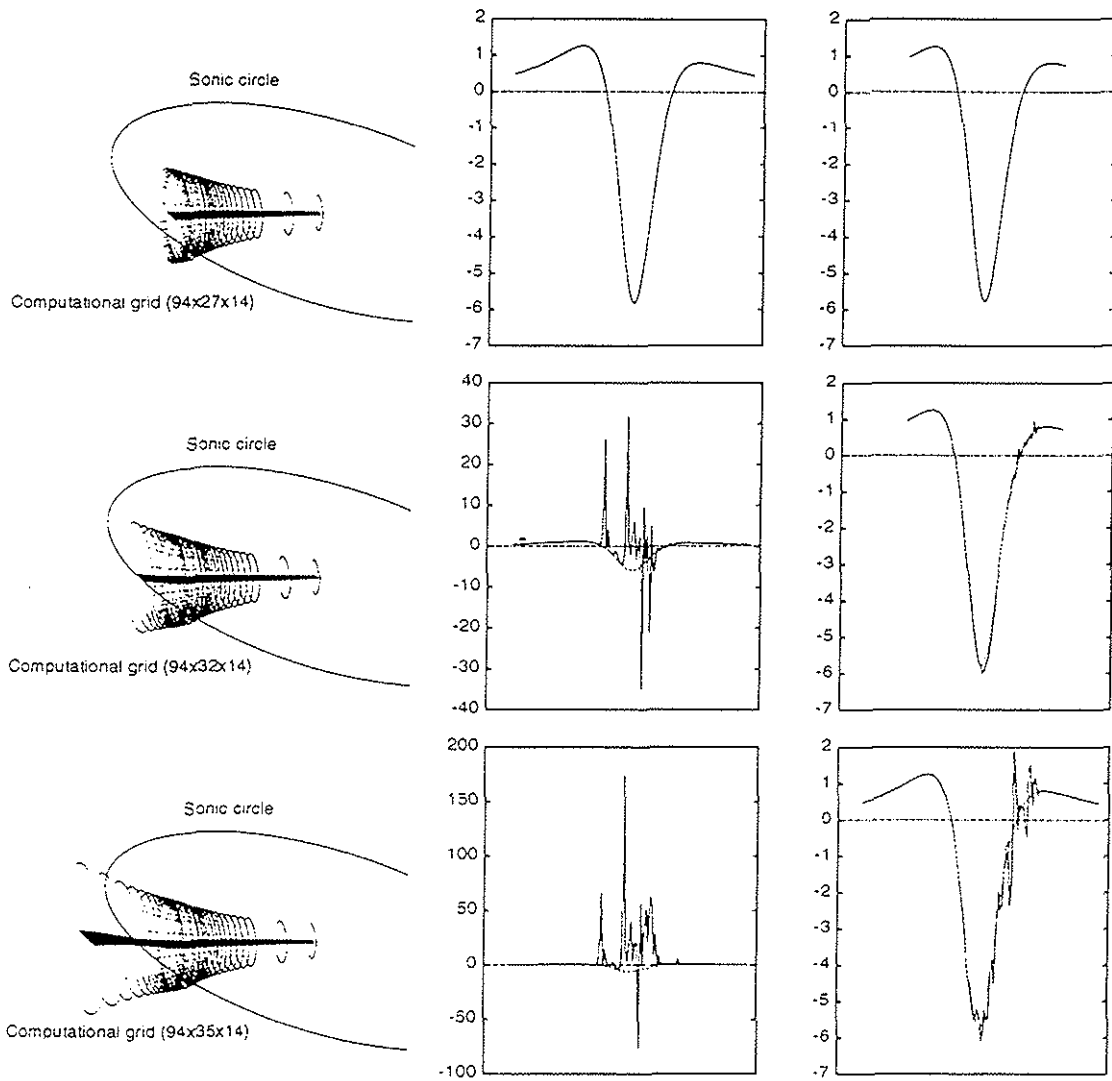


Figure 1 - Quadrupole noise signatures computed through the two different solution forms, for the hovering rotor blade at $M_{tip} = 0.8$, with different spanwise extensions of the numerical grid. Note the unreliability of noise predictions from equation (2) when the sonic circle is included in the computations (left figures), and the corresponding signatures obtained with the acoustic volume integration (right figures).

The particular test-case refers to a hovering rotor blade in lifting configuration, at a zero angle of attack but with a linear variation of the twist angle along span, with a tip Mach number of 0.8 and an observer location placed in the rotor plane, at $3.09R$ (with R equal to the blade radius). When the sonic

circle is included in the integration domain, the numerical prediction of noise from equation (2) becomes completely unreliable; on the contrary, the signatures computed through equation (3) come very close to the real acoustic pressure time history, in spite of some numerical instabilities which increase with the size of the grid's outer region.

These fluctuations are due to the lack of multiple emission times computation in the region outside the sonic circle and the subsequent wrong estimation of the outer grid volumes [2]. In fact, accounting for a supersonic zone causes the subdivision of the domain \mathcal{V} into three regions, corresponding to three different emission times for the supersonic source points. The shape and size of these particular regions depend on the fixed observer time and change at each time step; then, the evaluation of the integrals in the equation (3) may be achieved, establishing an ordered numbering system for the nodes of these supersonic regions.

3. The problem of multiple emission times

The determination of the emission time τ^* is achieved with an iterative procedure, solving the equation:

$$\tau = t - \frac{r}{c_0} = t - \frac{|\mathbf{x} - \mathbf{y}(\eta, \tau)|}{c_0} = \Phi(\tau) \quad (4)$$

where \mathbf{x} and \mathbf{y} represent the *present* and the *retarded* observer and source point positions, respectively, and η is the coordinate-vector of source point in the body frame of reference. Starting from the initial time $\tau = t$ and the corresponding positive value $f(\tau) = r/c_0$, the search for the roots of the function $f(\tau) = [\tau - \Phi(\tau)]$ proceeds backwards, with a prescribed time step $\Delta\tau$, up to the first sign inversion; then, the emission time τ^* is captured by subsequent iterations, until a specified error condition is satisfied. The shape of the $f(\tau)$ curve strongly depends on the rotational velocity and on the azimuthal position of source point with respect to the observer location. For a subsonic source point, the curve exhibits a single root, while a supersonic source point has two different points with a zero derivative; then, due to the angular position inside the revolution period, the curve may have more than a single sign inversion, usually leading to three different emission times.

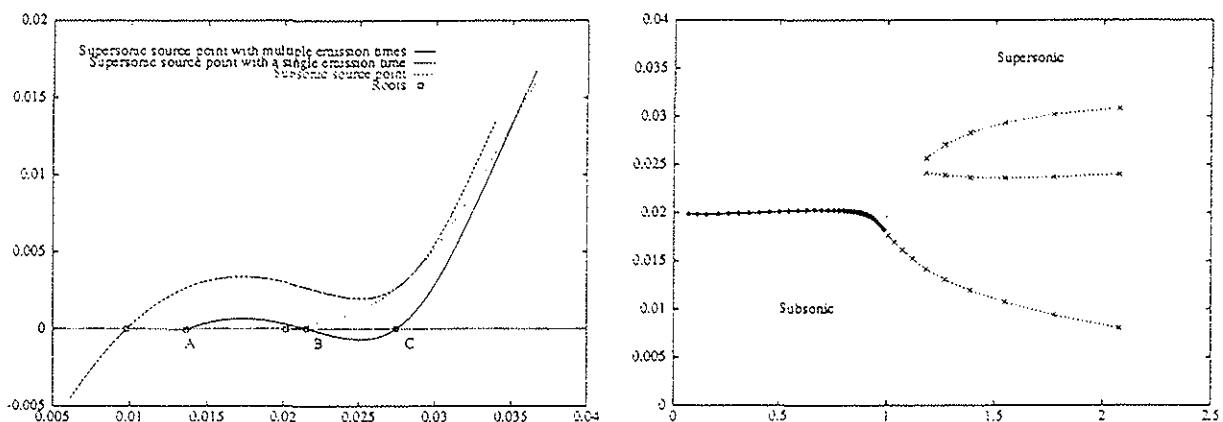


Figure 2 - On the left, the $f(\tau)$ curves at different rotational speed are shown. The right figure refers to the computed emission times for the blade trailing edge, at the different spanwise stations of the numerical grid: increasing the spanwise coordinate (or, in other words, the rotational Mach number), three different emission times arise.

This situation is clearly shown on the left of figure 2, where the function $f(\tau)$ is drawn for three source points at different rotational speed. On the right of the same figure, the computed emission times vs the rotational Mach number are shown for the blade trailing edge, at a given observer time: in the supersonic range the curve exhibits three different branches, due to the possible three emission times at some prescribed azimuthal position. The $f(\tau)$ curve provides many information about the emission times and the corresponding retarded positions of the source points. In fact, the possible three different roots for a supersonic source point are characterized by the subsequent time derivatives of the function itself, whose sign determines the retarded position within the revolution period. The first τ -derivative, $\partial f/\partial\tau = 1 - M_r$, exhibits a double sign inversion, related to the three different supersonic patches. The second patch (D2 in figure 3) is related to the second emission time (named B in figure 2); the particular position of these source points, for which the projection of the rotational Mach number in the source observer direction is greater than one, causes a pronounced noise generation. The other two regions always exhibit a M_r smaller than one, and are characterized by the sign of the second τ -derivative:

$$\frac{\partial^2 f}{\partial\tau^2} = M_i \hat{r}_i + \frac{c_0}{r} (M_r^2 - M^2) \quad (5)$$

related to the $f(\tau)$ curvature in the root-point. The solution of equation $\partial^2 f/\partial\tau^2 = 0$ has been numerically determined, and is shown in the figure 3, where the acoustic images of the first grid layer (including the blade) are shown at four different observer times. It is easily recognized that this solution is the inversion line for the acoustic surface curvature, which divides the space around the body into two separate regions, and clearly identifies the different supersonic patches related to the emission times A and C in figure 2 (named D1 and D3 in the figure 3).

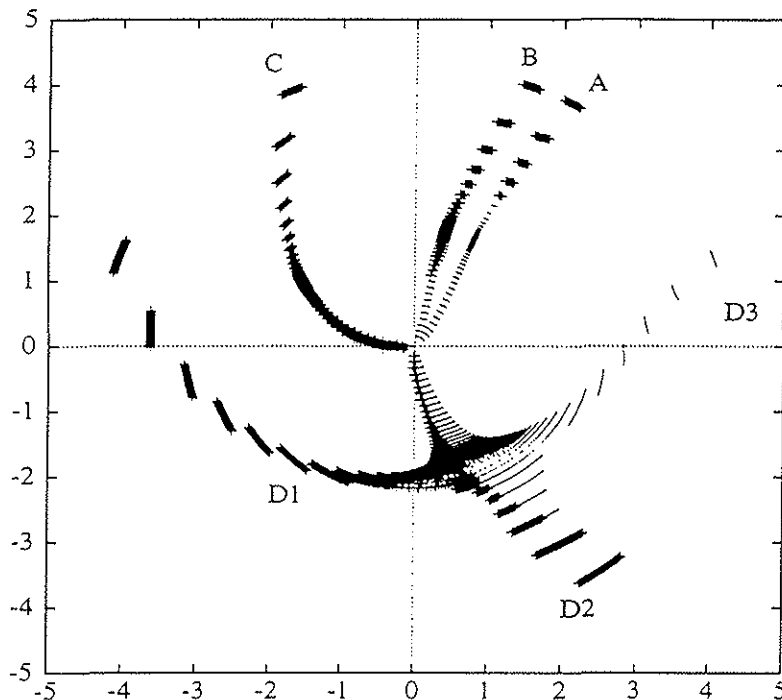


Figure 3 - The acoustic image of the first grid layer is shown at four different observer times. The passage from positive to negative values for the second τ -derivative $\partial^2 f/\partial\tau^2$ causes the inversion of the acoustic surface curvature.

The change in the acoustic surface curvature may be easily seen looking at the figure 4, where the emission times are reported versus the rotational Mach number (at a given observer time, with a high acoustic emission), for the blade leading and trailing edge, respectively. The trailing edge exhibits a positive second τ -derivative, and the *first* supersonic branch, constituting a continuous line with the subsonic region, is placed back to the other two supersonic branches. At the same observer time, the blade leading edge (corresponding to a negative value for $\partial^2 f / \partial \tau^2$), exhibits an opposite curvature, with the two separate supersonic branches back to the continuous subsonic-supersonic line.

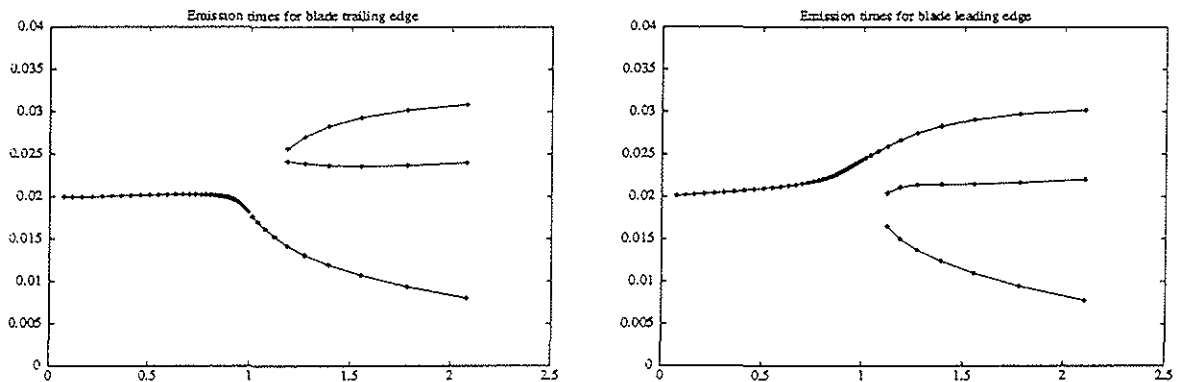


Figure 4 - These figures show the computed emission times vs the rotational Mach number, for the trailing edge (on the left) and the leading edge (on the right) of the rotor blade. The fixed observer time refer to the acoustic surface configuration named D in figure 3. Note the jump of the continuous subsonic-supersonic line, which characterizes the curvature inversion of the acoustic surface.

4. Numerical results

Once an ordered numbering system is established for the supersonic source points, the integration on the complete \mathcal{V} -domain may be performed. Due to the different number of source points on the upper and lower surfaces, and the subsequent changes of the supersonic patches (both in size and shape), it is necessary to adopt an interpolation scheme to evaluate the grid elementary volumes. In particular, it is possible to use a simple three dimensional and linear data-fitting routine to achieve a regular panelization of the supersonic patches; figure 5 shows the panelization performed for the second grid layer of the numerical domain, fixing 100 nodes chordwise upon each supersonic region. Since the numerical evaluation of equation (4) requires the computation *step-by-step* of all the retarded elementary volumes, it is possible to reduce the computing costs through the use of equation (3) inside the subsonic region. Then, the numerical code presently adopt both the solution forms, dividing the computational grid into two separate regions, on the grounds of a prescribed value of the rotational Mach number. Over a tip Mach number of 0.88 the quadrupole noise signature is characterized by a more and more pronounced asymmetrical shape and a *second* positive peak value, whose size strongly depends on the shock delocalization phenomena. The first numerical results obtained with the volume integration code for M_{tip} value in the high transonic range (over 0.88) seem to confirm these peculiarities, in spite of some pronounced fluctuations, whose nature is still to be investigated. This situation is clearly represented in figure 6, where the quadrupole noise signature from a hovering rotor blade at $M_{tip} = 0.9$ is determined through a decomposition of the computational domain into three separate regions. We point out the qualitative nature of these signatures, performed with only the first two grid layers of the computational domain. Of course, the

most significant contribution to the acoustic pressure field arises from region 2, included between the sonic circle and a rotational Mach number equal to 0.8. This value of the rotational speed has been assumed as the limit for the *actual* volume integration, where the noise prediction is achieved through equation (2); the acoustic signature computed for this zone is very small, exhibiting a typical symmetrical shape.



Figure 5 - The panel reconstruction as computed through a linear and three dimensional interpolation, fixing 100 nodes on the different grid layers. The retarded surface refers to a hovering rotor blade at $M_{tip} = 0.9$, at one of the highest acoustic emission times.

But the most interesting result refers to the integration performed upon the supersonic patches. Beside the expected increase of the negative peak value, the main effects of these particular regions on the overall acoustic pressure time history are an increase in the asymmetrical character of the resulting shape and the presence of some pronounced fluctuations placed in the recompression region, which seems to give rise to the typical second positive peak value. Actually, the full integration on the supersonic regions (considering all the computational grid layers), has provided a quite *dirty* signature, where the fluctuations affect all the resulting noise prediction; then, some numerical errors are probably related to them. However, the position and the size of these instabilities is always such as to produce a resulting shape very similar to the expected signature.

5. Why the volume integration?

The evaluation of the acoustic pressure field generated by rotating blades in transonic range is presently pursued with different numerical methods, mostly based on the so-called *Kirchhoff's* approach or the direct use of some CFD codes. Then, the application of the FW-H equation is usually limited to the evaluation of the linear terms only (thickness and loading noise). Anyhow, no plausible reason seems to justify this choice. The acoustic analogy approach is the only, real *acoustic* approach, able to provide an effective description of the acoustic phenomena taking place in the flow field. It establishes a clear relationship between each integral term and the different generating and propagating noise mechanisms, allowing an understanding and a deepening of the aeroacoustic problems, not achievable with the alternative, direct methods. For instance, the visualization of the blade retarded images during the revolution period, allows to understand how the geometry of the body affects the noise generation, suggesting a possible acoustic optimization of the blade shape, checked by the geometrical variations of the acoustic surface. The possibility to perform a separate integration upon some prescribed zones allows to evaluate

the contributions from particular regions of the numerical domain; in this manner, for example, the effects of a delocalized shock may be individually analysed and compared with the noise signature arising from a stronger shock wave, placed upon the blade surface.

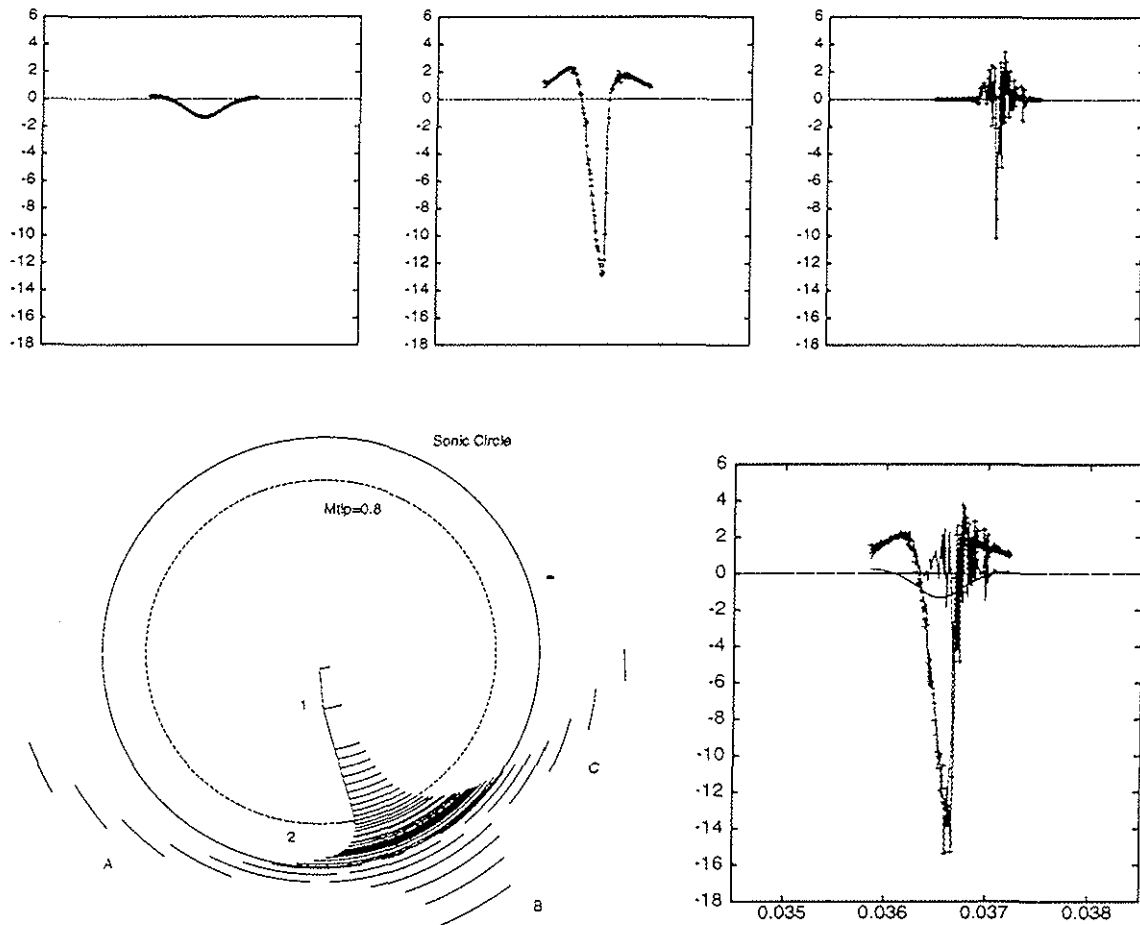


Figure 6 - The retarded image of the hovering rotor blade at $M_{tip} = 0.9$ is here reported at a prescribed observer time, characterized by a high sound emission. The top figures represent the different contributions arising from the separate integration regions. Note the pronounced asymmetrical shape of the resulting quadrupole noise signature and the position of the supersonic patches contributions, which give rise to the typical second positive peak value for the acoustic pressure.

Furthermore, the impulsive nature of the quadrupole noise signature may be exploited, in order to limit the computations to a particular azimuthal region. Then, the noise peak value may be found with few time steps (and a remarkable reduction of the requested CPU time), to identify the regions with the highest acoustic disturbances around the body, avoiding the computation of the overall acoustic pressure time history within the revolution period. These desirable results cannot be achieved with the use of an aerodynamic code, whose acoustic output has usually to be considered as a secondary outcome, and is forced to be the global acoustic pressure time history around the body. So, although the volume

integration always requires a set of aerodynamic data (being a pure *post-processor* of an aerodynamic input), it is certainly more suitable for the numerical treatment of the aeroacoustic problems, provided the computing costs are limited. Concerning the Kirchhoff's approach, its main advantage with respect to the Lighthill's analogy is the requirement for only a two dimensional integration, with a supposed reduction of the CPU time. Anyhow, different numerical problems are related to the choice of the integration domain and to the accuracy of the requested aerodynamic data; furthermore, some numerical singularities are still present in the numerical treatment of the supersonic regions. Consequently, if the computational effort is limited, the volume integration seems to be a valid alternative to the Kirchhoff's solution method.

Probably, the real weak-point of the volume integration is the availability of the requested aerodynamic data, involving the knowledge of the three dimensional fluid velocity field around the blade. This kind of information is very hard to be numerically found, and cannot arise from experimental test. Very good results, both for the resulting shape of the signatures and for the predicted negative peak values of the acoustic pressure, have been obtained up to a tip Mach number of 0.85, solving equation (2) and exploiting different sets of aerodynamic data (from an Euler and a full-potential, non-conservative code) [1, 2]. At present, our main effort is devoted to improve the integration on the supersonic regions, in view of further test-cases at higher rotational speed.

For many years the volume integration has not been used, since its application was considered too expensive, from a computational point of view, for the HSI noise prediction. Recently [2], it has been shown how some simple contrivances may be adopted to reduce the requested CPU time. With a suitable choice on the azimuthal region of interest and an optimized computation of the emission times, the converged solutions for the quadrupole noise signature presently require a CPU time varying between 15 and 30 minutes on a CONVEX C3860 System, depending on the size of the numerical domain (note that the double precision, which usually doubles the computing costs on this particular machine, has always been adopted in the calculations). These data do not yet include the calculation of multiple emission times and the integration on the supersonic regions, since they refer to tip Mach numbers smaller than 0.88; then, these values are certainly destined to grow. Anyhow, the CONVEX is generally considered four times slower than a CRAY-YMP, where the alternative solution methods require a largely comparable computational effort (80 minutes for the direct Euler solutions on the same hovering test-case [3], and 15 minutes for a forward flight test-case treated with the Kirchhoff's approach [9]). Furthermore, the use of a different integral solution, not based on the present simple zero-order formulation, and the adoption of some particular techniques, concerning a possible parallelization of the code, suggest some further enhancements in the requested CPU time. For these reasons we think it is no longer possible to disregard such a numerical approach for the aeroacoustic analysis of transonic tip speed blades.

6. Conclusions

The interesting and encouraging results achieved during one year of research activity on the volume integration, urge to some further developments of the methodology. The computational flexibility of the method and the proved effectiveness in the evaluation of HSI noise, make the acoustic analogy approach a very suitable tool for the aeroacoustic analysis of rotating blades, whose adoption cannot be limited to subsonic problems. Furthermore, the remarkable reduction achieved on the computing cost and the subsequent competitiveness compared to alternative methodologies, suggest the extension of the code for the numerical treatment of high speed propeller blades, where the supersonic region often includes part of the blade itself. A particular attention must be paid to the computing costs, whose size strongly affects the possibility of industrial applications: so, a continuing optimization work is to be considered in the development of the numerical procedure.

References

- [1] S. Ianniello and E. De Bernardis, Calculation of High Speed Noise from Helicopter Rotor Using Different Descriptions of Quadrupole Source, *AGARD Symposium on Aerodynamics and Aeroacoustics of Rotorcraft*, Berlin, Germany, 10-13 October 1994.
- [2] S. Ianniello and E. De Bernardis, Volume Integration in the Calculation of Quadrupole Noise from Helicopter Rotors, *First Joint CEAS/AIAA Conference*, Munich, Germany, 12-15 June 1995.
- [3] J.D. Baeder, J.M. Gallman and Y.H. Yu, A computational Study of the Aeroacoustics of Rotors in Hover, *American Helicopter Society 49th Annual Forum*, St. Louis, Missouri 1993.
- [4] G.R. Srinivasan and J.D. Baeder, Recent Advances in Euler and Navier-Stokes Methods for Calculating Helicopter Rotor Aerodynamics and Acoustics, *Fourth International Symposium on Computational Fluid Dynamics*, Davis, California, 9-12 September 1991.
- [5] J. Prieur, M. Costes and J.D. Baeder, Aerodynamic and Acoustic calculations of Transonic Non-lifting Hovering Rotors, *International Technical Specialists Meeting on Rotorcraft and Rotor Fluid Dynamics*, Philadelphia, Pennsylvania, 1991.
- [6] T.W. Purcell, R.C. Strawn and Y.H. Yu, Prediction of High-Speed Rotor Noise with a Kirchhoff Formula, *National Specialists Meeting on Aerodynamics and Aeroacoustics of AHS*, Arlington, TX, 1987.
- [7] T.W. Purcell, A Prediction of High-Speed Rotor Noise, *AIAA 12th Aeroacoustics Conference*, San Antonio, Texas 1989.
- [8] A.S. Lyrantzis, The use of Kirchhoff's Method in Rotorcraft Aeroacoustics, *AGARD Symposium on Aerodynamics and Aeroacoustics of Rotorcraft*, Berlin, Germany, 10-13 October 1994.
- [9] C. Polacsek and J. Prieur, High-Speed Impulsive Noise Computations in Hover and Forward Flight Using a Kirchhoff Formulation, *First Joint CEAS/AIAA Conference*, Munich, Germany, 12-15 June 1995.
- [10] F. Farassat, A New Theoretical Treatment for Propeller Noise, *Von Kàrmàn Institute Lecture Series 1981-82*, Brussels, Belgium, May 1982.